

1 Article

2 Preparation and Characterization of Two Types of 3 Tryptanthrin-Loaded Nanomicelles

4 Xin He [#], Qian Zhang [#], Youbei Qiao, Zhe Yu, Tiehong Yang ^{*} and Hong Wu ^{*}5 Department of Medicine Chemistry and Pharmaceutical Analysis, School of Pharmacy, the Fourth Military
6 Medical University, Xi'an 710032, China; 1543618464@qq.com7 [#] These authors contributed equally to this work.8 ^{*} Correspondence: wuhong@fmmu.edu.cn; Yangtiehong@fmmu.edu.cn

9 **Abstract:** Tryptanthrin has not been widely applied in clinical practice due to its poor solubility
10 and low bioavailability in spite of possessing several biological and pharmacological activities.
11 Here, to improve the solubility of tryptanthrin, two types of novel tryptanthrin-loaded micelles
12 were prepared. One was tryptanthrin physically encapsulated by distearoyl
13 phosphatidylethanolamine polyethylene glycol (DSPE-PEG) and the other was pegylated
14 tryptanthrin synthesized by acid-sensitive hydrazone bond and further prepared as micelles.
15 Molecular imprinting technology was used to separate pegylated tryptanthrin and free
16 mPEG-COOH in the preparation of PEGylated tryptanthrin micelles with considerably high
17 separation efficiency. The solubility of tryptanthrin-loaded DSPE-PEG micelles (TDMs) and
18 PEGylated tryptanthrin micelles (PTMs) was increased by 300 and 1493 fold compared with that of
19 tryptanthrin, respectively. The PTMs increased the solubility of tryptanthrin more effectively and
20 95% of tryptanthrin was released from PTMs at pH 5.5 in 12 h. The cytotoxicity of PTMs decreased
21 under physiological conditions compared with that of tryptanthrin, whereas at pH 5.5, the PTMs
22 showed comparable cytotoxicity with that of tryptanthrin, indicating successful drug release from
23 the carrier in response to tumor cell pH. Overall, we elucidated an efficient method to improve
24 water solubility of tryptanthrin and indicated pegylated tryptanthrin is a promising prodrug.

25 **Keywords:** nanomicelle; polyethylene glycol; tryptanthrin; water soluble

26

27 **1. Introduction**

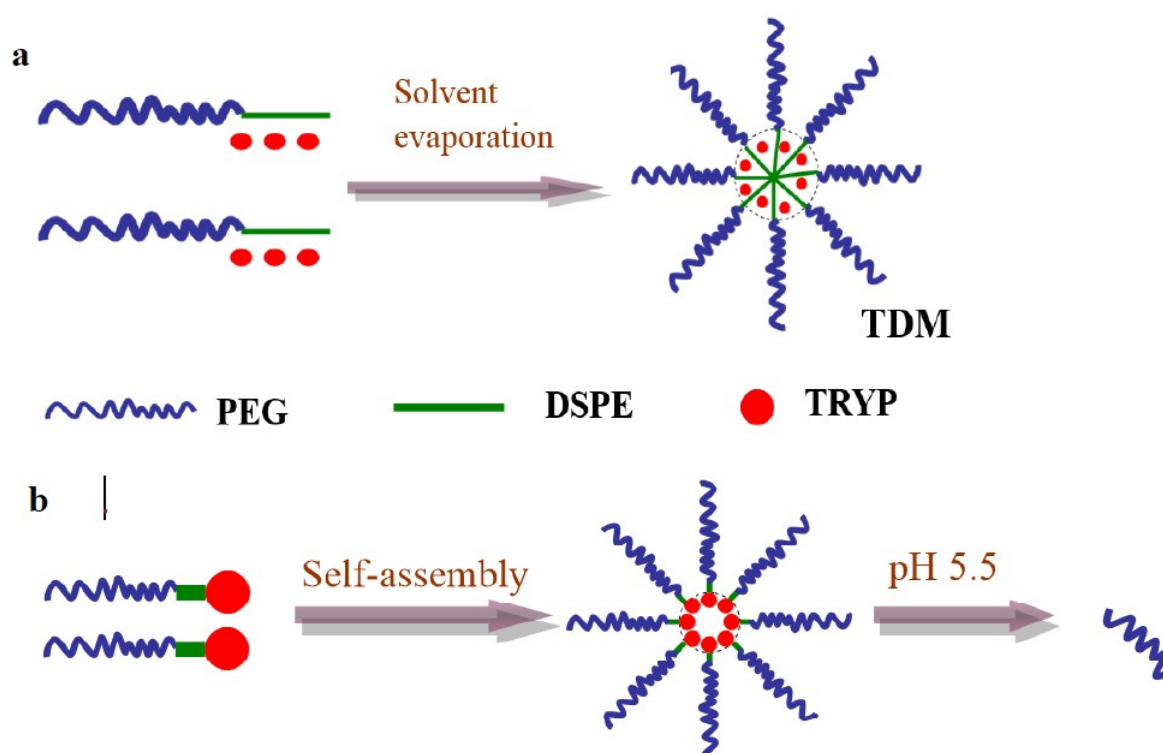
28 Tryptanthrin (TRYP), an indole quinazoline alkaloid, is a major active constituent extracted
29 from several Chinese herbal plants such as *Strobilanthes cusia*, *Polygonum tinctorium* Lour and
30 *Isatis tinctoria* [1,2]. It is reported that TRYP has a broad spectrum of biological activities including
31 anticancer, anti-inflammatory, antiprotozoal, antiallergic, and antimicrobial activities [3,4]. Our
32 previous study illustrated that TRYP has proliferation-attenuating and apoptosis-inducing effects on
33 a leukemia cell line *in vitro* and might be a new candidate to treat leukemia [5]. However, the poor
34 water solubility (1.339 µg/mL in water [6]) of TRYP limits its absorption in the body, resulting in its
35 extremely low bioavailability.

36 Liposomes and micelles [7-9] can increase the solubility of poorly soluble drugs, and they have
37 been extensively studied in recent years. The lipophilic drugs with the logarithms of oil/water
38 partition coefficient (P) (lgP) higher than 4.5 could be prepared as liposomes. Hence, TRYP with a
39 lgP of 2.37 [10] cannot form stable liposomes. Owing to the advantages of good solubilization
40 effect and simple production process, polymer micelles have garnered considerable attention [11,12].
41 Polymer micelles consist of hydrophobic cores and hydrophilic shells, and
42 polymer-drug-conjugated micelles (PDCM) are effective drug carriers that can be loaded with
43 hydrophobic drugs to increase solubility and bioavailability of the parent drug [13]. Besides, the
44 preparation process of polymer drug conjugate micelles is relatively simple, and drugs can be linked
45 to polymers by physical encapsulation or chemical binding [14], which greatly expands their range
46 of applications.

47 One of the polymers that is most commonly used in the preparation of polymer drugs is
 48 polyethylene glycol (PEG). Polyethylene glycol is an ideal drug carrier material and the Food and
 49 Drug Administration has approved PEG for human intravenous, oral, and dermal applications
 50 [15,16]. However, currently, most of the PEGylated drugs used in clinical practice are
 51 macromolecules and the key problem that restricts the application of PEGylated small-molecule
 52 drugs is the difficulty of separation of PEGylated drugs and free PEG. Because they have a similar
 53 molecular weight and polarity, the common column chromatography method is not applicable.
 54 Currently, the only small-molecule drug that is under clinical research is PEGylated irinotecan [17].

55 Molecular imprinting technology (MIT) has been widely applied in various fields to selectively
 56 separate target molecules because of its recognition specificity and application universality [18,19].
 57 MIT was innovatively applied for the separation of PEGylated TRYP and mPEG-COOH of similar
 58 molecular weight in our work.

59 In order to improve the solubility of TRYP, two types of TRYP-loaded micelles were prepared
 60 in this study. The first method was encapsulating TRYP with DSPE-PEG. Amphiphilic DSPE-PEG
 61 was used to form micelles by employing the solvent evaporation method and hydrophobic TRYP
 62 was encapsulated in it (Figure 1a). The second method was to connect TRYP and PEG through
 63 hydrazone bonds. The amphiphilic block copolymer, TRYP-PEG, was used to form micelles by
 64 employing the dialysis method (Figure 1b).



65
 66 **Figure 1.** Schematic diagram of TDMs (a) and PTMs (b).

67 2. Materials and Methods

68 2.1. Materials

69 Unless stated otherwise, all reagents were obtained from commercial sources and were
 70 analytical grade. TRYP was a gift from department of Natural medicine, the Fourth Military Medical
 71 University. Distearoyl phosphatidylethanolamine -[methoxy (polyethylene glycol)-2000]
 72 (DSPE-PEG₂₀₀₀) was purchased from Ruixi BioEngineering Inc. Methoxy polyethylene glycol
 73 (molecular mass 2000 Da, purity >95%) was purchased from Nanocs(America). Acetonitrile (ACN)

74 was purified through 0.22 μm membrane. Distilled deionized water was produced using the Millpak
 75 Reagent Water System (Millipore, USA). Pyrene, Dicyclohexylcarbodiimide (DCC),
 76 4-dimethylaminopyridine (DMAP), acrylamide, ammonium persulfate, 2-hydrazinoethanol, and
 77 N,N-dimethylacrylamide were purchased from Sigma Aldrich (USA). DMEM medium and CCK-8
 78 were purchased from KeHao BioEngineering Inc.

79 2.2. Preparation and verification of TRYP-loaded DSPE-PEG micelles

80 DSPE-PEG₂₀₀₀ (44.29 mg) and TRYP (100 mg) were dissolved in 30 mL of trichloromethane.
 81 After the removal of solvent by rotary evaporation and desiccation, a thin film was acquired. It was
 82 dissolved in phosphate buffer solution and passed through hydrophilic membrane filters (0.45 μm).
 83 The filtrate contained only TRYP-loaded DSPE-PEG micelles (TDMs).

84 The encapsulation of TRYP was verified by proton nuclear magnetic resonance (¹H NMR). The
 85 NMR spectra were obtained using Varian 400MHz (Bruker, Germany), with tetramethylsilane (TMS)
 86 as the internal standard. Chemical shifts are expressed as parts per million (ppm). TRYP and
 87 DSPE-PEG₂₀₀₀ (10 mg) were dissolved in 0.6 mL of CDCl₃. Thereafter, two equal parts of TDMs (10
 88 mg) were dissolved in D₂O and CDCl₃, respectively.

89 2.3 Synthesis of TRYP-PEG

90 Tryptanthrin (248 mg, 1 mmol) was dissolved in 25 mL of tetrahydrofuran (THF) and
 91 2-hydroxyethyl hydrazine (76 mg, 1 mmol) was dissolved in 3 mL of ethanol. The mixture was
 92 stirred at room temperature under nitrogen atmosphere for 12 h. The reaction process was
 93 monitored by thin layer chromatography (TLC) on F254 silica gel pre-coated sheets (Qing Dao,
 94 China) and the products were purified by column chromatography.

95 mPEG₂₀₀₀-COOH (40 mg, 0.02 mmol), TRYP-NNHCH₂CH₂OH (6.12 mg, 0.02 mmol),
 96 4-dimethylaminopyridine (DMAP, 22.3 mg, 0.183 mmol), and dicyclohexylcarbodiimide (DCC, 26.5
 97 mg, 0.136 mmol) were dissolved in 15 mL of dry dichloromethane, and then the solution was stirred
 98 in an ice bath for 24 h. The impurities were removed and the crude product was acquired by suction
 99 filtration. The unreacted mPEG-COOH was removed using PEG-imprinted polymer that was
 100 prepared as mentioned below.

101 2.4. Preparation and adsorption of imprinted polymer

102 mPEG-COOH (100 mg, 0.05 mmol), acrylamide (3.55 mg, 0.05 mmol), and N,N-
 103 dimethylacrylamide (39.6 mg, 0.4 mmol) were dissolved in 30 mL of distilled water. The solution
 104 was then stirred at room temperature for 30 min. Thereafter, ammonium persulfate (100 mg, 0.44
 105 mmol) was added and the solution was placed in an oil bath at 85°C under vigorous stirring with
 106 reflux condensation for 12 h. Ten microliters of anhydrous ethanol was added to the product and the
 107 mixture was transferred to centrifuge tubes. The sample was centrifuged at 12000 rpm for 10 min,
 108 and then the supernatant was discarded and the precipitate was resuspended in ethanol.
 109 Centrifugation was repeated under the same condition three times or more. The supernatants were
 110 collected; the absorbance of the supernatant was detected using a UV spectrophotometer
 111 (MAPADA, Shanghai, China). When mPEG-COOH could not be monitored, washing was stopped.
 112 The collected precipitates contained imprinted polymers, with mPEG-COOH as the template
 113 molecule (PEG molecularly imprinted polymers, PMIPs).

114 To measure the adsorption performance of PMIPs, 4 mL of 0.2 mg/mL mPEG-COOH solution
 115 was added to 11 mg of PMIPs. The sample was placed in a constant temperature (25°C) shaker at 100
 116 rpm, and then subjected to full wavelength scanning by ultraviolet spectrophotometry at 200–300
 117 nm after 30 min. The process was repeated, except that the mPEG-COOH solution was replaced by
 118 TRYP-PEG solution of the same concentration. The changes in absorbance were observed and the
 119 adsorption rate of PMIPs to PEG or TRYP-PEG was calculated using the following equation.

$$120 \quad \text{Adsorption rate (mg/g)} = \frac{\text{total mass of material} - \text{mass of unadsorbed material}}{\text{total mass of PMIPs}}$$

121 2.5. Characterization of TRYP-PEG

122 The synthesized polymers TRYP-PEG were confirmed by ^1H NMR. TRYP-PEG was dissolved
123 in 0.5 mL of D_2O . Fourier transformed infrared spectroscopy (FTIR) was also used to confirm the
124 structure of TRYP-PEG. The spectra were obtained using the Nicolet 5DXC IR spectrometer
125 (Nicolet, Madison, USA) at a resolution of 2 cm^{-1} and a spectral range of $4000\text{--}400\text{ cm}^{-1}$. The sample
126 was ground with KBr into a fine powder.

127 2.6 Drug-release study

128 The in vitro drug-release profile was determined using a dynamic dialysis method. Briefly,
129 TRYP-PEG was incubated with phosphate-buffered saline (PBS) solution of different pH (pH 5.5
130 and 7.4). Typically, 5 mL of TRYP-PEG solution (2 mg/mL) was dialyzed (MWCO: 1 kDa) against 25
131 mL of PBS solution at 100 rpm in a constant temperature shaker at 37°C . At predetermined intervals
132 (0.5, 1, 2, 3, 6, 9, and 12 h), 1 mL of external buffer was removed and an equal volume of PBS solution
133 was refilled. The concentration of TRYP released from polymeric micelles was quantified by
134 ultraviolet spectrophotometry at 251 nm.

135 As PEG is a large molecule and unfavorable for a chromatographic column, to investigate
136 fracture behavior of hydrazone bond and drug release, the structural change in
137 TRYP-NNHCH₂CH₂OH instead of TRYP-PEG was studied under acidic conditions.

138 In brief, 0.5 mg of TRYP-NNHCH₂CH₂OH was dissolved in 4 mL of acetic acid solution (pH 5.5)
139 for 30 min. The samples, TRYP, TRYP-NNHCH₂CH₂OH, and TRYP-NNHCH₂CH₂OH in acetum, were
140 detected by thin layer chromatography, and the developing solvent used was ethyl
141 acetate-petroleum ether (50:50, v/v).

142 High performance liquid chromatography (HPLC) was used to detect the three samples
143 further. Chromatographic separation was carried out on the Agilent 1260 Infinity LC system
144 (Agilent, Germany). Assay was conducted using a C18 column (200 mm × 4.5 mm, 5 μm particle
145 size) under isocratic elution with acetonitrile–water (47:53, v/v). The flow rate was 0.8 mL/min and
146 the injection volume was 10 μL. The detection wavelength was 251 nm and the column temperature
147 was maintained at 25°C .

148 2.7 Preparation of PEGylated TRYP micelles

149 TRYP-PEG (4.3 mg) was dissolved in 2 mL of DMSO. The solution was stirred rapidly for 2 h,
150 and then 10 mL of deionized water was added dropwise into the solution. The solution was stirred
151 slowly for 12 h, and then transferred into a pretreated dialysis bag (MWCO: 1 kDa) and dialyzed
152 against deionized water. The outer phase was replaced with fresh deionized water every 3 h. After
153 12 h, the PEGylated TRYP micelles (PTMs) were obtained and stored at 4°C for further use.

154 2.8 Determination of solubility

155 The solubility of TDMs and PTMs was measured according to the method of general rules of
156 Chinese Pharmacopoeia (2015). The TDMs and PTMs were freeze dried before the experiment. To 1
157 g of TDMs and PTMs, an appropriate amount of PBS (pH 7.4) was added at 25°C and shaken for 30 s.
158 Then, PBS was added dropwise until there were no insoluble substance, and then the volume of PBS
159 was measured and solubility was calculated.

160 2.9 Particle size distribution of TDMs and PTMs

161 The particle size distribution of the micelles was evaluated by dynamic light scattering (DLS)
162 using the Delsa™ Nano C Particle analyzer (BECKMAN Coulter Instruments, USA). The
163 morphology of polymeric micelles was observed using a transmission electron microscope (TEM,
164 JEM-1230, Japan).

165 2.10 Critical micellar concentration determination

166 The critical micelle concentration (CMC) was estimated by fluorescent spectroscopy [20].
167 Pyrene (10 mg) was dissolved in 25 mL of acetone (1×10^{-5} mol/L). The micelle samples were
168 dispersed in PBS (pH 7.4) at a concentration range of 1–10 $\mu\text{g/mL}$. Then, 20 μL of pyrene solution
169 was evaporated in dark to remove the solvent, and 2 mL of polymer solutions of different
170 concentrations was added. The mixed solutions were ultrasonically shaken for 1 min. After 12 h, the
171 fluorescence values were measured. The excitation wavelengths were set at 335 nm. The fluorescent
172 intensity at 373 and 384 nm were measured and the ratio of them was calculated. The CMC of
173 micelles was determined from the inflection points in the fluorescent intensity ratios versus micelles
174 concentration curves.

175 2.11 Tumor cell line and cell culture

176 Human breast tumor cell line MCF-7 was cultivated in DMEM supplemented with 10% fetal
177 calf serum and 1% antibiotics (containing penicillin and streptomycin) in a humidified 5% $\text{CO}_2/95\%$
178 air atmosphere at 37°C .

179 2.12 *In vitro* cytotoxicity test

180 The *in vitro* cytotoxicity of TRYP- $\text{NNHCH}_2\text{CH}_2\text{OH}$ and TRYP-PEG was investigated using the
181 Cell Counting Kit-8 (CCK-8) assay. The cells were seeded into 96-well culture plates at a density of 5
182 $\times 10^4$ cells per well and incubated at 37°C for 24 h. Then, the corresponding culture medium was
183 replaced by 200 μL of DMEM medium containing TRYP and PTMs at different concentrations under
184 different pH (7.4 and 5.5). After incubating for another 48 h, 10 μL of CCK-8 solution was added to
185 each well of the plate and the cells were incubated for 2 h at 37°C . Cell viability was determined by
186 scanning using the Bio-Rad 680 microplate reader at 450 nm.

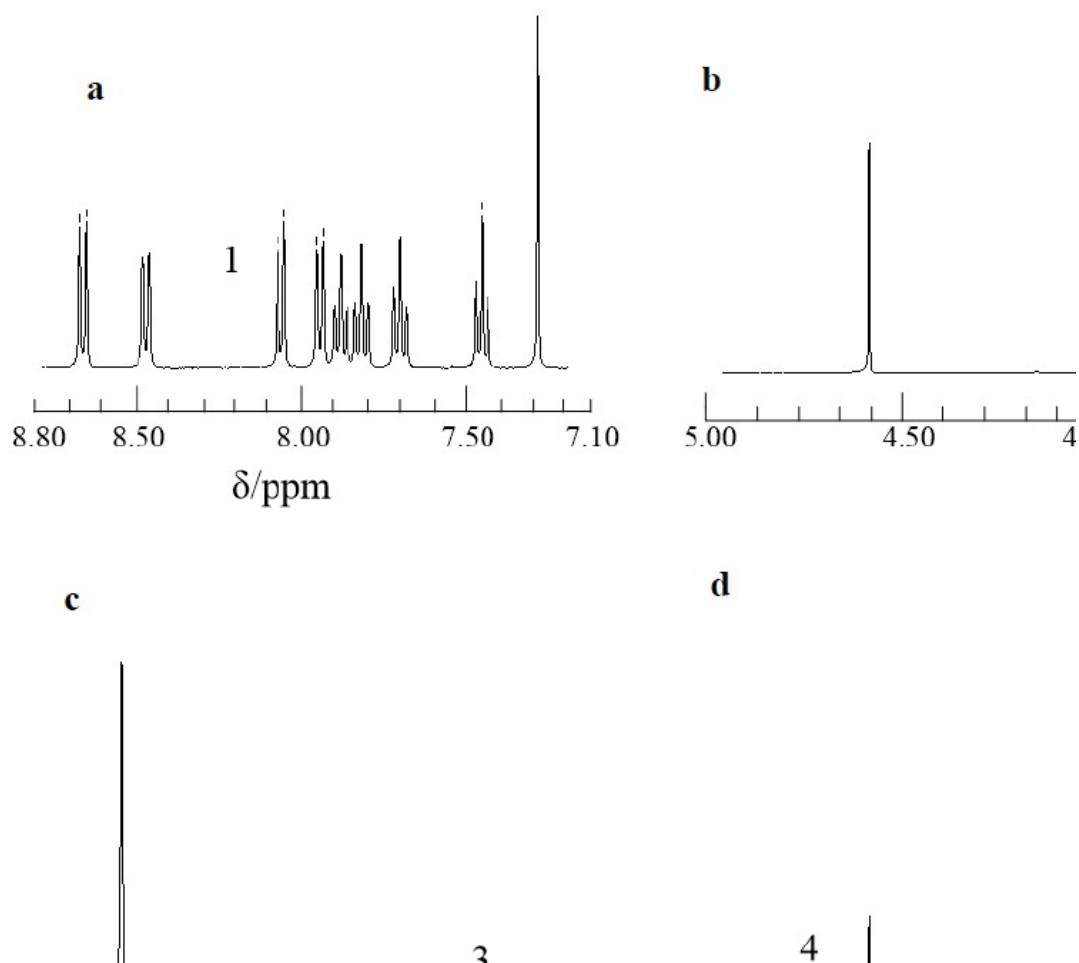
187 2.13 Statistical analysis

188 The results are presented as mean \pm standard deviation of at least three repetitive experiments
189 for all the treatment groups. Statistical analysis was conducted using the one-way ANOVA with
190 Student's *t*-test using a SPSS 23.0 program; $P < 0.05$ indicated significant difference.

191 3. Results and Discussion

192 3.1. Preparation and verification of TDMs

193 As reported, the characteristic peaks of tryptamine were at δ 8.42 ppm (d), δ 7.66 ppm (t), δ 7.84
194 ppm (t), δ 8.02 ppm (d), δ 7.90 ppm (d), δ 7.42 ppm (t), δ 7.78 ppm (t), and δ 8.62 ppm (d), and PEG
195 compounds presented large peaks around δ 3.6–3.7 ppm, which can be ascribed to repeated $-\text{CH}_2$
196 groups of the PEG chains [21]. The shell of TDMs was hydrophilic, and therefore, the micelle was
197 stable in aqueous solution and tryptamine was encapsulated in the core of the micelle. Therefore, the
198 characteristic peaks of tryptamine did not appear in the spectrum presented in Figure 2c. On the
199 contrary, the “core-shell” structure of micelle was broken by trichloromethane and TRYP was
200 exposed as shown in Figure 2d. The results of ^1H NMR verified the encapsulation of TRYP.



201
 202 **Figure 2.** ¹H-NMR spectra of TRYP (a), DSPE-PEG₂₀₀₀ (b), TDMs dissolved in D₂O (c), and TDMs dissolved in
 203 CDCl₃ (d).

204 3.2. Preparation and characterization of TRY-P-PEG

205 The synthetic route of TRY-P-PEG is illustrated in Figure 3a. Hydrophilic flexible chain
 206 (polyethylene glycol) was introduced into TRY-P by pH-sensitive hydrazone bond. Pegylated TRY-P
 207 was obtained by a two-step reaction. Firstly, TRY-P was modified by 2-hydroxyethyl hydrazine and
 208 the pH-sensitive hydrazone bond was introduced at C6 of TRY-P. Therefore, the intermediate
 209 product TRY-P-NNHCH₂CH₂OH was obtained. The reaction conditions were mild and the products
 210 were purified by column chromatography. Then, TRY-P-PEG was obtained by esterification between
 211 the carboxyl groups of PEG and hydroxy groups of TRY-P-NNHCH₂CH₂OH. The excess mPEG was
 212 removed by molecular imprinting and a pure product was obtained.

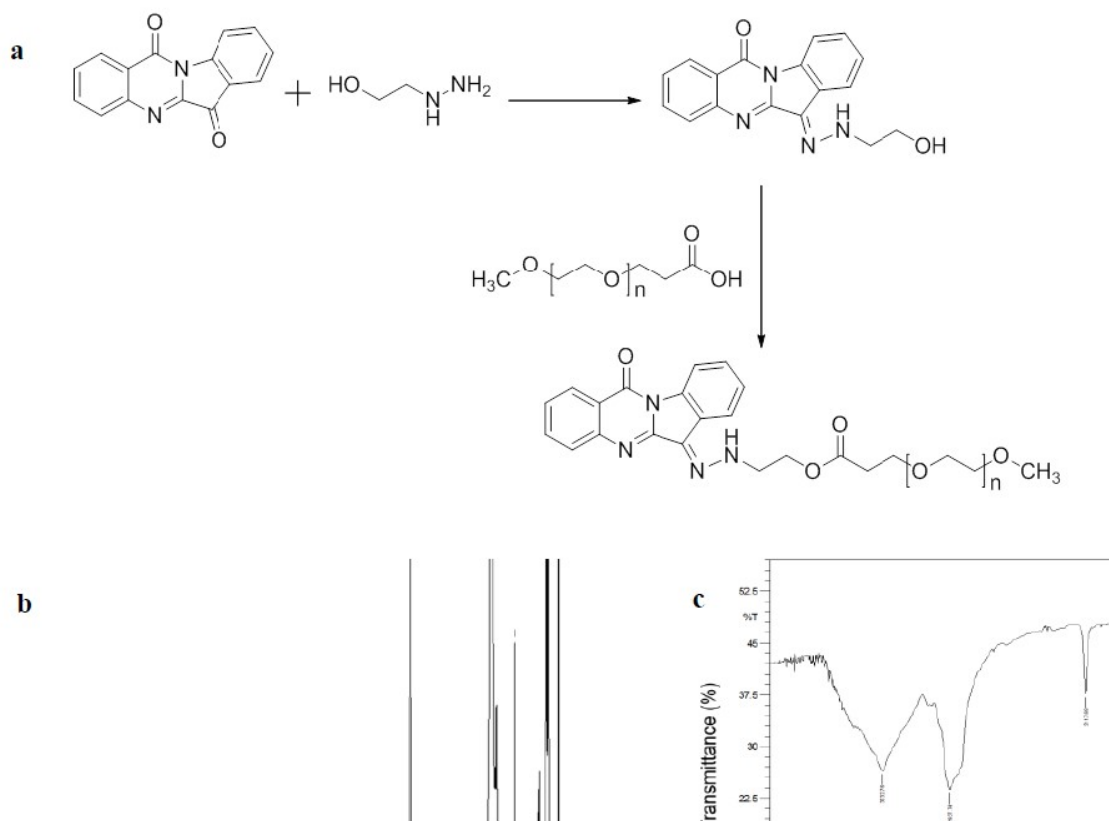


Figure 3. Synthetic route (a), ¹H-NMR spectra (b), and FTIR spectra (c) of TRYP-PEG.

213

214

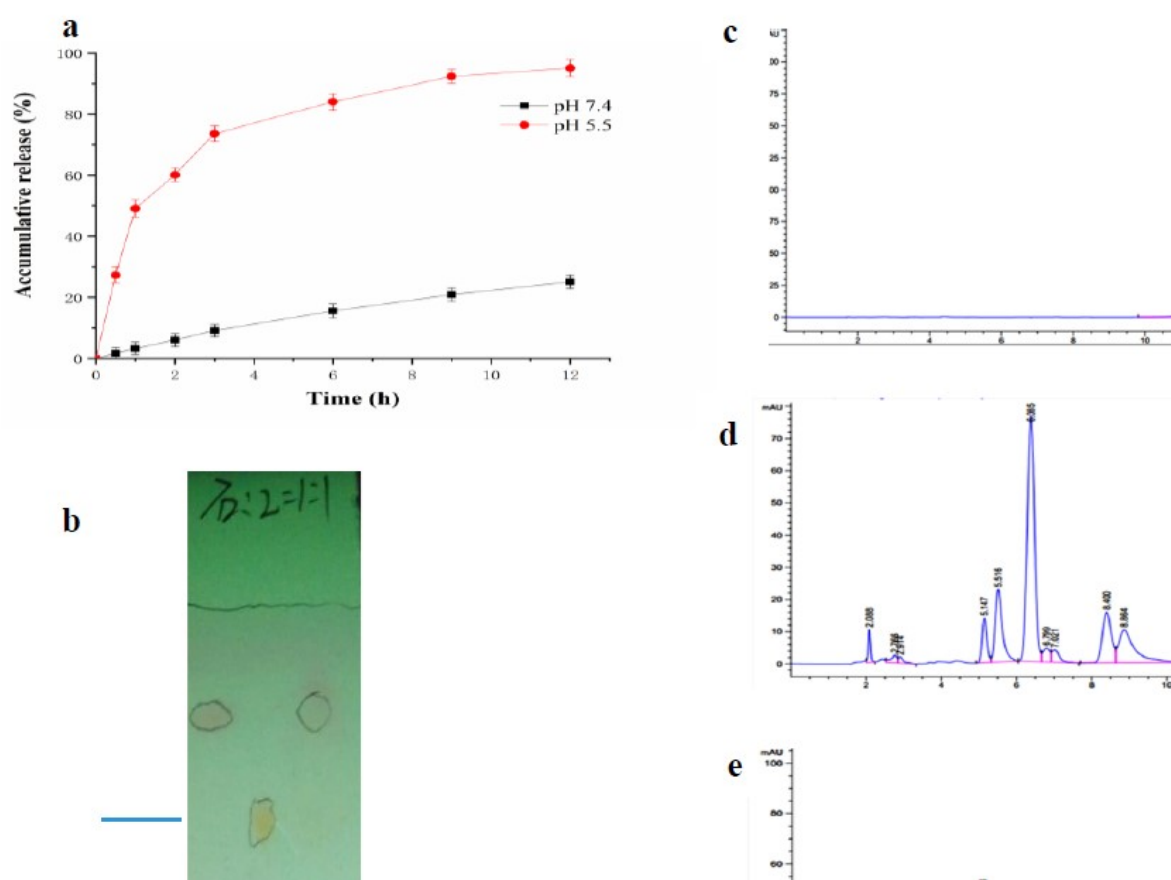
215 The chemical structure of TRYP-PEG was characterized by ¹H-NMR and FTIR. As shown in
 216 Figure 3b, the characteristic peak of both TRYP (δ 7.4–8.4 ppm) and PEG (δ 3.6 ppm) was observed,
 217 which proved that PEG was conjugated to TRYP successfully. As shown in Figure 3c, the spectra of
 218 TRYP-PEG presented new absorption peaks at 1095 cm⁻¹ (C-O-C stretching vibration) and 1778 cm⁻¹
 219 (C=O stretching vibration). The appearance of characteristic peaks of PEG and ester group verified
 220 the successful synthesis of TRYP-PEG.

221 3.3. Adsorption experiments of imprinted polymer

222 The adsorption capacity of PMIPs to mPEG-COOH and TRYP-PEG was evaluated by UV-vis
 223 spectrophotometry. The adsorption rates of PMIPs to mPEG-COOH and TRYP-PEG were 520 and
 224 7.3 mg/g, respectively. The adsorbability of PMIPs to mPEG-COOH was 71 times higher than that of
 225 TRYP-PEG, showing that through molecular imprinting, mPEG-COOH could be absorbed by
 226 PMIPs efficiently, which indicated that excess mPEG-COOH could be separated from TRYP-PEG
 227 effectively and relatively pure TRYP-PEG could be obtained.

228 3.4. Drug-release study

229 The release of TRYP from TRYP-PEG was measured to confirm the pH sensitivity of drug
 230 release. The in vitro TRYP-release amount was investigated at different pH (pH 7.4 and 5.5). As
 231 shown in Figure 4a, the release of TRYP was negligible at pH 7.4 with an accumulative release
 232 profile of 25% in 12 h, indicating that the hydrazone bond was relatively stable under physiological
 233 conditions. However, as the pH decreased from 7.4 to 5.5, there was an increase in the release of
 234 TRYP and approximately 95% of TRYP was released in 12 h. It was obvious that the release of TRYP
 235 was pH dependent, and the drug was released rapidly and completely under acidic conditions,
 236 which will enable the application of the drug against tumor.



238

239 **Figure 4.** Accumulative release profiles of TRYP from TRYP-PEG under different pH (n = 3) (a). TLC
 240 chromatogram of TRYP, TRYP-NNHCH₂CH₂OH, and TRYP-NNHCH₂CH₂OH in acetum (b). HPLC of TRYP
 241 (c), TRYP-NNHCH₂CH₂OH (d), and separated product of TRYP-NNHCH₂CH₂OH in acetum for 30 min (e).

242 TRYP-NNHCH₂CH₂OH was stable in PBS (PH 7.4). However, in acidic solution, hydrazone
 243 bond was cracked and TRYP was released. As shown in Figure 4b, after incubation with acetum for
 244 30 min, the spot of TRYP- NNHCH₂CH₂OH disappeared, whereas a new spot was observed in the
 245 TLC plate, and its retardation factor (R_f) was the same as that of TRYP.

246 High performance liquid chromatography was used to further analyze the substance. Peaks of
 247 TRYP (t_R = 11.39min) and TRYP- NNHCH₂CH₂OH (t_R = 15.85 min) were observed in the spectra
 248 presented in Figure 4c and 4d, respectively. As shown in Figure 4e, after incubation with acetum for
 249 30 min, a peak of TRYP (t_R = 11.39min) appeared, which indicated the disruption of hydrazone bond
 250 and release of TRYP.

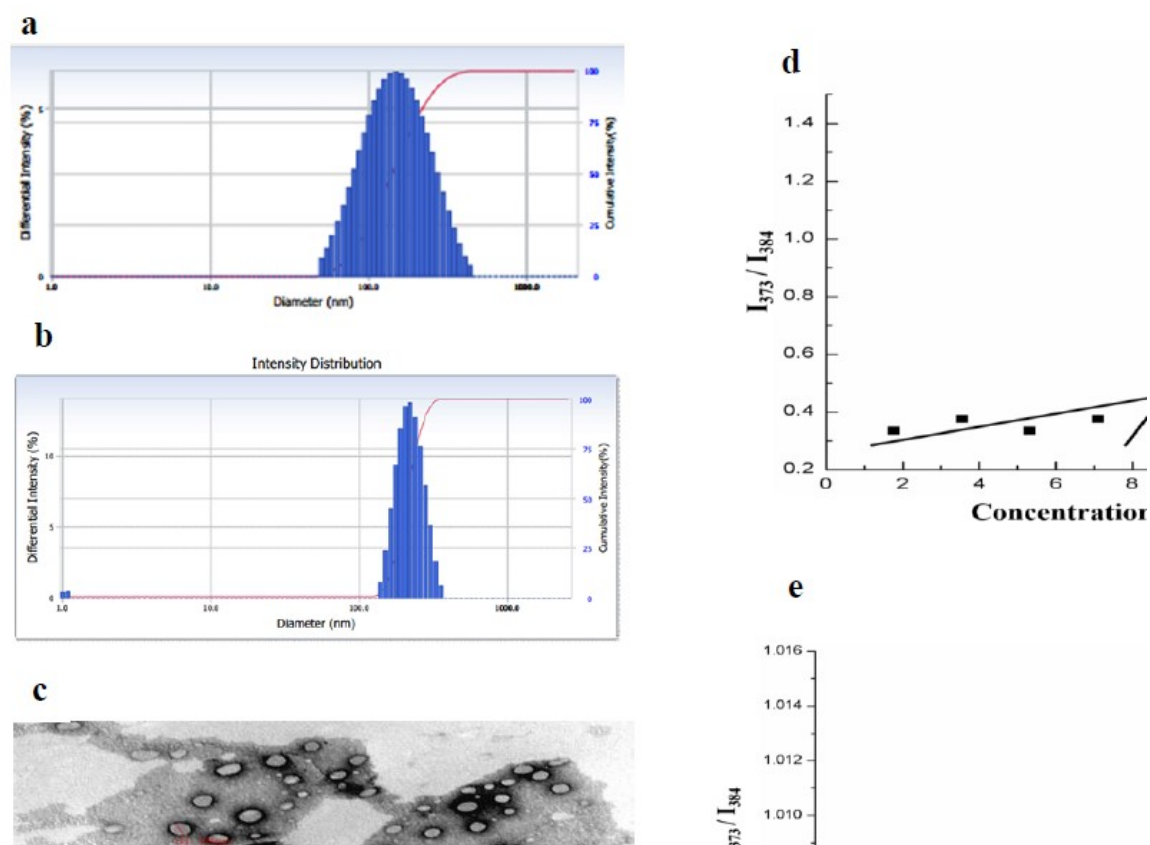
251 3.5. Solubility in aqueous solution

252 The solubility of TRYP in TDMs and PTMs was 1.625 and 8.065 mmol/L, respectively, which
 253 was around 300- and 1493-fold higher than that of TRYP (1.339 μg/mL in aqueous solution),
 254 indicating the strong solubilizing ability of PEG. The application of TRYP has been studied more and
 255 more, however, there is only little research on improving its solubility [22]. Our study provided a
 256 relatively simple but effective way to improve the solubility of TRYP.

257 Furthermore, it is apparent that the method of preparing micelles by chemical bonding could
 258 increase the solubility of TRYP more effectively than physical encapsulation, therefore the PTMs
 259 were chosen for further analyses.

260 3.6. Particle size distribution of TDMs and PTMs

261 The TDMs were prepared using the solvent evaporation method, with a particle size of 112.5 nm and
 262 PDI of 0.15 (Figure 5a). The PTMs were prepared using the dialysis method, with a particle size of
 263 228.8 nm and PDI of 0.1 (Figure 5b). The morphology of PTMs was examined by TEM. As shown in
 264 Figure 5c, the micelles were spherical with an average diameter of 50 nm, which was considerably
 265 smaller than the particle size measured by DLS. It was probably because the DLS analysis provided
 266 dynamic diameter in aqueous solution, which was larger than the size of dried particles.



267
 268 **Figure 5.** Particle size and distribution of TDMs (a) and PTMs (b). TEM of PTMs (c). CMC of TDMs
 269 (d) and PTMs (e).

270 The CMC of TDMs and PTMs was 8.93×10^{-6} and 3.5×10^{-7} mol/L, respectively (Figure 5d and
 271 5e). The low CMC indicated the high stability of prepared micelles and facilitated further use; both
 272 of them were stable.

273 3.7. Cytotoxicity test

274 In vitro cytotoxicity of TRYP and PTMs against MCF-7 cells was studied using the CCK-8 assay.
 275 Figure 6 shows the viability of MCF-7 cells incubated with different concentrations of TRYP or PTMs
 276 for 48 h. The pH of 7.4 and 5.5 was selected to simulate the normal physiological condition and
 277 tumor site acidic condition, respectively.

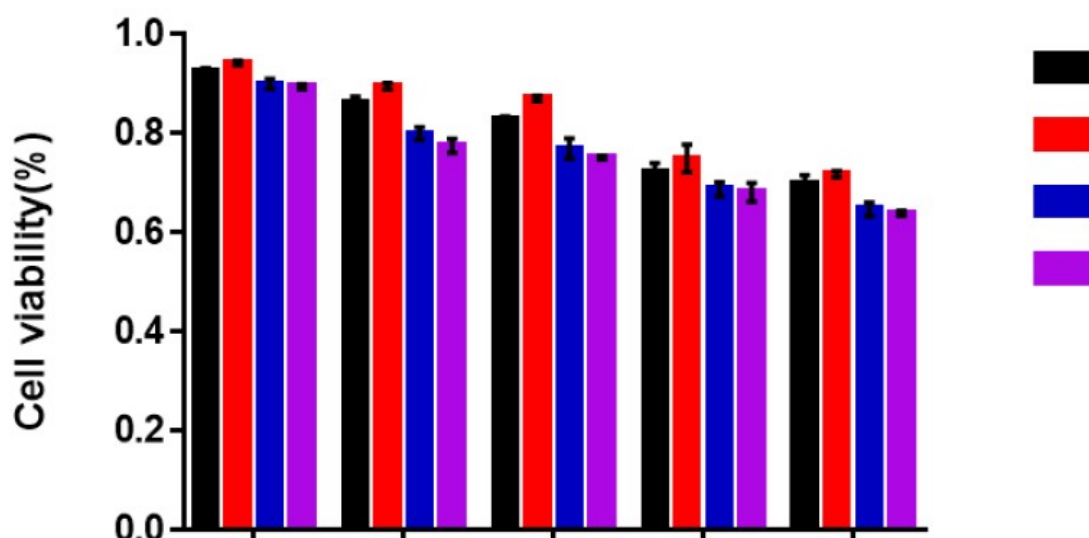


Figure 6. Cytotoxicity of TRYP and PTMs on MCF-7 cells at different pH (7.4 and 5.5).

278

279

280 As shown, both drug and PTMs showed concentration-dependent toxicity. The viability of
 281 MCF-7 cells decreased with the increase in the concentration of TRYP or PTMs. The viability of
 282 PTM-treated cells was higher than that of TRYP-treated cells at pH 7.4 ($P < 0.05$), which indicated
 283 that the cytotoxicity of PTMs was reduced compared with that of TRYP under normal physiological
 284 conditions. This may be due to the stability of TRYP when prepared as micelles. The PTMs exhibited
 285 the same cytotoxicity at pH 5.5, which indicated that PTMs had activity comparable to that of TRYP
 286 under acidic conditions.

287 Combined with previous study results, that is, the TRYP-release rate from micelles was higher
 288 under acidic conditions and the pH of tumor microenvironment is significantly higher than that of
 289 normal tissues, the PTMs have potential use as an antitumor agent.

290 5. Conclusions

291 There have been more and more application studies of TRYP, however, only little research on
 292 increasing its solubility. Herein, we report two novel strategies to improve the solubility of TRYP.
 293 The solubility of TRYP in TDMs and PTMs was increased by 300 and 1493 fold compared with that
 294 of TRYP, respectively, making it possible for it to be used effectively. Besides, both these micelles
 295 had relatively low CMC, which indicated the high stability of prepared micelles and facilitated their
 296 further use.

297 The PTMs could improve the solubility of TRYP more obviously; therefore, these micelles were
 298 chosen for further research. The drug release from PTMs was pH dependent. The complex exhibited
 299 stability under physiological conditions and the drug-release rate was extremely low; however,
 300 TRYP was almost completely released within 12 h at pH 5.5, which was propitious for drug release,
 301 and exerted the pharmacological action under acidic condition. Moreover, compared with the parent
 302 drug TRYP, the cytotoxicity of PTMs decreased at pH 7.4, which indicated that the cytotoxicity of
 303 PTMs was reduced under normal physiological conditions. Whereas at pH 5.5, the PTMs showed
 304 comparable cytotoxicity with TRYP. The results indicated that these nanomicelles could be applied
 305 as an anti-tumor agent.

306 In this study, the preparation of TRYP as nanomicelles improved the solubility of TRYP, which
 307 lays a foundation for further improvement in its bioavailability and application of anti-tumor.

308 **Author Contributions:** H. W. conceived and designed the experiments; X. H., Q. Z. and Y.Q.
 309 performed the experiments; X. H. and Q. Z. analyzed the experimental data; Z.Y. made the graphics;
 310 X. H. wrote the paper; H. W. and T. Y. reviewed and edited the paper.

311 **Funding:** This research was funded by the National Natural Science Foundation of China (Grant No.
312 81571786, 31771087, 31671015).

313 **Conflicts of Interest:** The authors declare no conflict of interest.

314 References

- 315 1. Kaur, R.; Manjal, S.K.; Rawal, R.K.; Kumar, K. Recent synthetic and medicinal perspectives of
316 tryptanthrin. *Bioorganic & medicinal chemistry* **2017**, *25*, 4533-4552, doi:10.1016/j.bmc.2017.07.003.
- 317 2. Pedras, M.S.C.; Abdoli, A.; To, Q.H.; Thapa, C. Ecological Roles of Tryptanthrin, Indirubin and
318 N-Formylanthranilic Acid in *Isatis indigotica*: Phytoalexins or Phytoanticipins? *Chemistry & biodiversity*
319 **2019**, *16*, e1800579, doi:10.1002/cbdv.201800579.
- 320 3. Olson, J.A.; Terryn, R.J., 3rd; Stewart, E.L.; Baum, J.C.; Novak, M.J. New insight into the action of
321 tryptanthrins against *Plasmodium falciparum*: Pharmacophore identification via a novel submolecular
322 QSAR descriptor. *Journal of molecular graphics & modelling* **2018**, *80*, 138-146,
323 doi:10.1016/j.jmgm.2017.12.013.
- 324 4. Han, N.R.; Moon, P.D.; Kim, H.M.; Jeong, H.J. Tryptanthrin ameliorates atopic dermatitis through
325 down-regulation of TSLP. *Archives of biochemistry and biophysics* **2014**, *542*, 14-20,
326 doi:10.1016/j.abb.2013.11.010.
- 327 5. Miao, S.; Shi, X.; Zhang, H.; Wang, S.; Sun, J.; Hua, W.; Miao, Q.; Zhao, Y.; Zhang, C.
328 Proliferation-attenuating and apoptosis-inducing effects of tryptanthrin on human chronic myeloid
329 leukemia K562 cell line in vitro. *International journal of molecular sciences* **2011**, *12*, 3831-3845,
330 doi:10.3390/ijms12063831.
- 331 6. Lipinski, C.A. Drug-like properties and the causes of poor solubility and poor permeability. *Journal of*
332 *pharmacological and toxicological methods* **2000**, *44*, 235-249, doi:10.1016/s1056-8719(00)00107-6.
- 333 7. Daeihamed, M.; Dadashzadeh, S.; Haeri, A.; Akhlaghi, M.F. Potential of Liposomes for Enhancement
334 of Oral Drug Absorption. *Current drug delivery* **2017**, *14*, 289-303,
335 doi:10.2174/1567201813666160115125756.
- 336 8. Upponi, J.R.; Jerajani, K.; Nagesha, D.K.; Kulkarni, P.; Sridhar, S.; Ferris, C.; Torchilin, V.P. Polymeric
337 micelles: Theranostic co-delivery system for poorly water-soluble drugs and contrast agents.
338 *Biomaterials* **2018**, *170*, 26-36, doi:10.1016/j.biomaterials.2018.03.054.
- 339 9. Bilia, A.R.; Piazzini, V.; Risaliti, L.; Vanti, G.; Casamonti, M.; Wang, M.; Bergonzi, M.C. Nanocarriers:
340 A Successful Tool to Increase Solubility, Stability and Optimise Bioefficacy of Natural Constituents.
341 *Current medicinal chemistry* **2019**, *26*, 4631-4656, doi:10.2174/0929867325666181101110050.
- 342 10. Hwang, J.M.; Oh, T.; Kaneko, T.; Upton, A.M.; Franzblau, S.G.; Ma, Z.; Cho, S.N.; Kim, P. Design,
343 synthesis, and structure-activity relationship studies of tryptanthrins as antitubercular agents. *Journal*
344 *of natural products* **2013**, *76*, 354-367, doi:10.1021/np3007167.
- 345 11. Yu, G.; Ning, Q.; Mo, Z.; Tang, S. Intelligent polymeric micelles for multidrug co-delivery and cancer
346 therapy. *Artificial cells, nanomedicine, and biotechnology* **2019**, *47*, 1476-1487,
347 doi:10.1080/21691401.2019.1601104.
- 348 12. Liu, Z.; Wang, Y.; Zhang, N. Micelle-like nanoassemblies based on polymer-drug conjugates as an
349 emerging platform for drug delivery. *Expert opinion on drug delivery* **2012**, *9*, 805-822,
350 doi:10.1517/17425247.2012.689284.
- 351 13. Ling, L.; Ismail, M.; Du, Y.; Xia, Q.; He, W.; Yao, C.; Li, X. High Drug Loading, Reversible Disulfide
352 Core-Cross-Linked Multifunctional Micelles for Triggered Release of Camptothecin. *Molecular*
353 *pharmaceutics* **2018**, *15*, 5479-5492, doi:10.1021/acs.molpharmaceut.8b00585.
- 354 14. Kesharwani, S.S.; Kaur, S.; Tummala, H.; Sangamwar, A.T. Multifunctional approaches utilizing
355 polymeric micelles to circumvent multidrug resistant tumors. *Colloids and surfaces. B, Biointerfaces* **2019**,
356 *173*, 581-590, doi:10.1016/j.colsurfb.2018.10.022.
- 357 15. Arpicco, S.; Stella, B.; Schiavon, O.; Milla, P.; Zonari, D.; Cattel, L. Preparation and characterization of
358 novel poly(ethylene glycol) paclitaxel derivatives. *International journal of pharmaceutics* **2013**, *454*,
359 653-659, doi:10.1016/j.ijpharm.2013.05.027.
- 360 16. D'Souza A, A.; Shegokar, R. Polyethylene glycol (PEG): a versatile polymer for pharmaceutical
361 applications. *Expert opinion on drug delivery* **2016**, *13*, 1257-1275, doi:10.1080/17425247.2016.1182485.
- 362 17. Fiorentini, G.; Carandina, R.; Sarti, D.; Nardella, M.; Zoras, O.; Guadagni, S.; Inchingolo, R.; Nestola,
363 M.; Felicioli, A.; Barnes Navarro, D., et al. Polyethylene glycol microspheres loaded with irinotecan for
364 arterially directed embolic therapy of metastatic liver cancer. *World journal of gastrointestinal oncology*
365 **2017**, *9*, 379-384, doi:10.4251/wjgo.v9.i9.379.

- 366 18. Chen, L.; Wang, X.; Lu, W.; Wu, X.; Li, J. Molecular imprinting: perspectives and applications. *Chem*
367 *Soc Rev* **2016**, *45*, 2137-2211, doi:10.1039/c6cs00061d.
- 368 19. Bossi, A.; Bonini, F.; Turner, A.P.; Piletsky, S.A. Molecularly imprinted polymers for the recognition of
369 proteins: the state of the art. *Biosensors & bioelectronics* **2007**, *22*, 1131-1137,
370 doi:10.1016/j.bios.2006.06.023.
- 371 20. Santos, A.P.; Panagiotopoulos, A.Z. Determination of the critical micelle concentration in simulations
372 of surfactant systems. *The Journal of chemical physics* **2016**, *144*, 044709, doi:10.1063/1.4940687.
- 373 21. Krivogorsky, B.; Nelson, A.C.; Douglas, K.A.; Grundt, P. Tryptanthrin derivatives as *Toxoplasma*
374 *gondii* inhibitors--structure-activity-relationship of the 6-position. *Bioorganic & medicinal chemistry*
375 *letters* **2013**, *23*, 1032-1035, doi:10.1016/j.bmcl.2012.12.024.
- 376 22. Fang, Y.P.; Lin, Y.K.; Su, Y.H.; Fang, J.Y. Tryptanthrin-loaded nanoparticles for delivery into cultured
377 human breast cancer cells, MCF7: the effects of solid lipid/liquid lipid ratios in the inner core. *Chemical*
378 *& pharmaceutical bulletin* **2011**, *59*, 266-271, doi:10.1248/cpb.59.266.